Scientific paper

Determination of Trace Cr(VI) with Diphenylcarbazide by μFIA–Thermal Lens Microscopy

Tatyana Gor'kova,[1,2] Mingqiang Liu,[1] Mikhail Proskurnin[2,*] and Mladen Franko[1]

[1] *University of Nova Gorica, Laboratory for Environmental Research, Nova Gorica 5000, Slovenia*

[2] *Analytical Chemistry Division, Chemistry Department, Lomonosov Moscow State University, Moscow 119991, Russia*

** Corresponding author: E-mail: proskurnin@gmail.com; Fax +7-495-939-4675*

Received: 26-04-2016

Abstract

The optimum reaction parameters for the interaction of hexavalent chromium [Cr(VI)] with diphenylcarbazide in microfluidic chips (μFIA) with thermal-lens microscopic detection were selected. The characteristic feature of the applied flow scheme is the injection of the reagent into the stream containing the test metal, which enables in-field and real-time monitoring of Cr(VI) simply by flowing the sample continuously through the microchip. The limit of detection of Cr(VI) under the selected conditions (signal generating wavelength, 514.5 nm; excitation power, 100 mW; detection position, 10 cm downstream from the mixing zone of the microchip; flow rate 10 μL min^{-1}; injection volume, 1.4 μL) is 15 ng mL^{-1} (2.9×10^{-7} mol L^{-1}). The linear range is 40 ng mL^{-1} – 10 μg mL^{-1} with a relative standard deviation no higher than 10% in the concentration range 0.1–1 μg mL^{-1}. The online monitoring by this scheme provides the possibility of up to 360 analyses per hour.

Keywords: Photothermal lensing; thermal-lens microscopic detection; microfluidic applications; μFIA; hexavalent chromium; diphenylcarbazide

1. Introduction

The interest for trace chromium analysis appears from its essential bioactivity and toxicity. Recently, several papers dealt with its importance as a biomarker, especially cardiomarker, and genotoxicity.[1–4] Currently available novel methods for trace Cr(VI) determination rely on chromium speciation based on ion chromatography, high-performance liquid chromatography or solid phase or liquid-liquid extraction coupled to atomic absorption and emission spectrometry or ICP-MS,[5–11] To avoid the need for separation of Cr(III) and Cr(VI) selective reagents were proposed, which react selectively with Cr(VI), such as rhodamine B hydrazide for spectrofluorimetric detection,[12] or well known diphenylcarbazide for spectrophotometric determination, which was recently significantly improved in sensitivity by using long-path-length molecular absorption spectroscopy, or optical waveguide sensors.[13–16] However, there are several problems of the determination of trace amounts of this metal–production monitoring in environmental analysis,[17] cosmetic industry,[18] rapid clinical diagnostics,[19] several problems of sports medicine[20] – require rapid monitoring or (and) speciation analysis, which cannot be implemented by these techniques. Moreover, solving these problems require developing compact instruments and tests providing the possibilities of rapid and mobile analysis and diagnostics with high sensitivity (at the level of 10–100 nmol L^{-1} or lower[1,2] but without stationary in-laboratory equipment for example in the case of ICP–AES and ICP–MS.

Towards this aim, microfluidic technologies are a very versatile platform for such analysis. They enable working with small sample amounts in an automatic flow mode and can be implemented as flow-injection analysis, chromatography, or electromigration.[21–24] In this study, we selected microflow-injection analysis (**μFIA**) as it provides the highest throughput of analysis and simplicity of the implementation.

As a detection method, the selection of thermal lensing (**TL**) as a tool for very sensitive detection of light absorption[25,26] is a very reliable option. Another

reason for the selection of a thermal lens technique is that compact analytical instruments in the variant of thermal lens microscopy, TLM,[27,28] were already introduced.

For the determination of chromium in a microfluidic chip with TLM, we selected the well-known photometric reaction of the formation of colored chelate of Cr(VI) with diphenylcarbazone (DPC). This reaction provides high sensitivity along with a very simple design of a flow microchip – only two flows may be used, the test solution and the reagent in a protolytic buffer solution. Moreover, the maximum of the absorption band of the formed Cr(VI)–DPC chelate (540 nm) lies near the wavelength of the most frequently used excitation lasers in TLM, which provides high instrumental sensitivity of the detection. The DPC method for Cr(VI) determination is well established and results for analysis of various samples were previously reported in literature, including the detection in a batch-mode TLS and for flowing systems such as ion-chromatography-TLS. TLS determinations of chromium were performed in good agreement with other methods such as atomic-absorption spectroscopy.[29–33] Also, the possibility of FIA-TLM for the determination of Cr(VI) was shown by a classical scheme of the injection of the test solution into a flow of a preconditioned reagent,[34] which showed high sensitivity of thermal-lens measurements and the applicability of the method. However, the problems of rapid assessment like in express analysis or in clinical diagnostics,[22,23] such a variant is not-optimal due to high flow rate of the reagent, or washout of the test samples after their injection into the reagent flow.

The aim of this paper is to develop an alternative variant of μFIA-TLM for determination of Cr(VI): the injection of the preconditioned reagent into a continuous or discrete flow of the test solution. We estimated the analytical performance parameters of this mode and compared them with the existing data.[34]

2. Experimental

In TLM used in this work, an excitation (pump) beam from an argon-ion laser (514.5 nm, Innova 90, Coherent Inc. USA) is modulated by a mechanical chopper at 1.03 kHz, and then is combined by a dichroic mirror with a probe beam from a He–Ne laser (632.8 nm, 25-LHP-151-230, Melles Griot, Rochester, USA) (more details are described previously[35]). The two beams are aligned coaxially through an objective lens (20 × /NA 0.45), and further through a microchip, where the TL effect is generated in the sample under the excitation by the pump beam (4 μm in diameter at its waist). The probe beam (2 μm in diameter at its waist) is diffracted by the thermal-lens effect and then its axial intensity is monitored by a photodiode (PDA36A, Thorlabs, USA) behind an interference filter and a 4-mm pinhole. TL signals are extracted by a lock-in amplifier (SR830, Stanford Research Systems, USA) and further recorded by a computer. Two types of microchips were used in this work: a microchip with a 205 μm wide × 100 μm deep microchannel (Dolomite Microfluidics, UK) – referred to as N1 and N2 – a microreactor chip with a 220-μm wide × 50-μm deep microchannel (Micronit Microfluidics, Enschede, The Netherlands). A microsyringe pump (NE-1000, New Era Pump Systems Inc., Farmingdale, USA) on which a 250-μL syringe was mounted is used to inject a certain amount of the reagent (DPC) instantly into the microchannel at a flow rate of 200 μL min^{-1}. Another microsyringe pump of the same type with a 5-mL syringe is employed to drive the sample containing Cr(VI) through the microchannel at a certain flow rate. The carrier containing the sample flows through the microchip continuously while the reagent is injected in a pulsed mode. The generated Cr(VI)–DPC was detected online by TLM at certain position downstream from the junction point.

Water from a Milli Q water purification system (Millipore, France) was used: specific resistance 18.2 MΩ × cm, Fe, 2 pg mL^{-1}; dissolved SiO_2, 3 ng mL^{-1}; total ion amount, < 0.2 ng mL^{-1}; TOC, < 10 ng mL^{-1}. The glassware was washed with acetone followed by conc. nitric acid. Nitric (69%), and hydrochloric (37%) acids, both of PA-ACS-ISO grade (Panreac, Spain) were used. The reagents: potassium dichromate ($K_2Cr_2O_7$, Riedel–de Haën, Germany), 1,5-diphenylcarbazide (DPC, CAS no. 140-22-7, Sigma–Aldrich), 1,10-phenanthroline iron(II) sulfate complex (ferroin, 0.025 mol L^{-1}, CAS No. 140-22-7, Sigma–Aldrich), phosphoric acid (H_3PO_4, 85%, Riedel–de Haën) and acetone (HPLC grade, J. T. Bakers) were used throughout. All the reagents and solvents used in this study were of chemically pure grade or higher and were used without further purification.

A stock standard solution (1 mg mL^{-1}) of Cr(VI) was prepared by dissolving 2.8 mg of $K_2Cr_2O_7$ in 1 mL of doubly deionized water. Sample solutions of lower concentration (25, 50, 100, and 200 ng mL^{-1}) were prepared by appropriate dilution. A stock solution of DPC was prepared by dissolving 2 mg of DPC in 1 mL of acetone. A H_3PO_4 solution was prepared by diluting 0.6 mL of 85% H_3PO_4 with 1.4 mL of water. A DPC reagent solution (5 mL) for online generation of Cr(VI)–DPC was prepared by diluting 0.4 mL of the DPC stock solution with 4.4 mL of water and 0.2 mL of diluted H_3PO_4.

In experiments, the reagent injection volumes of 0.1–1.44 μL, flow rates of 1–50 μL min^{-1} for carrier flow (corresponding to flow velocities of 0.2–10 cm s^{-1} in the microchannel), and pump laser powers of 1–125 mW were used to investigate the influence of these factors on the μFIA–TLM signal as well as the effects of photodegradation of Cr(VI)–DPC complex. The measurement results are presented in accordance with the requirements of ISO/IEC 17025:2005.[36]

3. Results and Discussion

In the work, we used the TLM spectrometer with geometry of the optical scheme optimized,[37] and only the day-to-day calibration by the iron(II) *tris*(1,10-phenanthrolinate) (ferroin) solution (1×10^{-5} mol L^{-1}) was made prior to each measurement session. We optimized the following experimental parameters of thermal-lens detection and the reaction conditions altogether: excitation laser power (*Ð*), carrier flow rate (*q*), sample-injection volume (*V*), and the thermal-lens detection position at the microchip (D_p).

Excitation power and the carrier flow rate (*q*) determines the sensitivity and the photobleaching of the Cr(VI)–DPC complex, while other parameters (D_p and *V*) in combination with the flow rate *q* affect only the completeness of the reaction of formation of the target chelate at the detection point.

The preliminary experiments are made with a simple flow-through microchip, N1 with pre-synthesized Cr(VI) chelate. This microchip was selected due to its simplicity and convenience of the work (Fig. 1, a). The major part of the work for selecting the reaction conditions and the estimation of the performance parameters was made using a N2 microchip with a double-Y geometry, and with a much longer microchannel (over 25 cm) after the junction point of carrier and reagent channels (Fig. 1, b), which makes the optimization of analytical parameters (*q*, *V*, and D_p) possible, and was specially designed for the target flow-injection analytical systems.

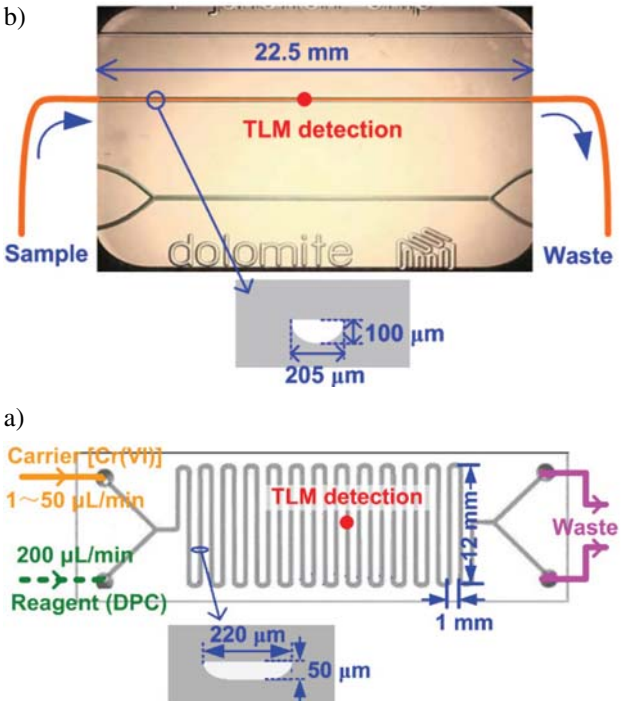

Figure 1. Schematic diagrams of (a) continuous flow analysis on microchip N1 and (b) microfluidic-FIA on microchip N2, with indicated TLM detection points. See the text for details.

3. 1. The Effect of the Excitation Power

At the first stage of experiments, we estimated the effect of the excitation laser power as it sets the sensitivity level of thermal lensing as a power-based method.[27] However, Cr(VI)–DPC chelate is not photostable under prolonged sample irradiation (e.g. for serial analyses in FIA-TLS). Thus, in the case of μFIA–TLM, the measurement time should be optimized to account for or to exclude photobleaching of the target chelate.[34]

In the case of FIA-TLS, the fluence of the excitation laser for a beam waist of 30 μm and a power of 100 mW is 3.5×10^3 W cm^{-2}; the irradiation time is *ca.* 0.1 s (the test solution flows through a cell with an optical path length of 1 cm and a volume of 8 μL, for a chopper frequency of 30 Hz and a flow rate of 2.5 mL min^{-1}. In the case of μFIA–TLM, for an optical path length of 2 μm and the same excitation power, the fluence is 8×10^5 W cm^{-2}, which would significantly affect the measurement results.

The effect of the excitation power on the target chelate was studied in the range of 2–125 mW. In a continuous-flow mode (only a sample flow goes through a measurement channel), we targeted the pre-synthesized Cr(VI)–DPC chelate with a known concentration. For comparison sake, we made similar experiments with ferroin as a substance a priori photostable under the selected conditions. All the experiments were carried out at flow rates of 5, 15, and 30 μL min^{-1}. Signal ratios for both substances and different flow-rate pairs are summed up in Table 1; the dependences of the thermal-lens signal on the excitation power are shown in Fig. 2.

The data shows that in all the selected range of excitation powers, the signal dependence is linear and in a good agreement with the theoretically expected behavior. The signals for all the three pairs of flow rates for Cr(VI)–DPC are very close to the expected ratios for photostable ferroin (Table 1), which is an evidence of a low degree of photobleaching of the target chelate. Thus, in all the following experiments, we used an excitation power of 100 mW.

Table 1. The ratios of slopes derived from dependences of thermal-lens signal on the excitation power (Fig. 2) calculated for flow rate pairs of 15 and 5, 30 and 5, and 30 and 15 μL min^{-1} for pre-synthesized Cr(VI)–DPC chelate and ferroin ($n = 3$, $P = 0.95$)

First/Second flow rate (μL min^{-1})	Cr(VI) chelate with DPC	Ferroin
15/5	1.03 ± 0.03	1.00 ± 0.03
30/5	0.96 ± 0.03	0.93 ± 0.03

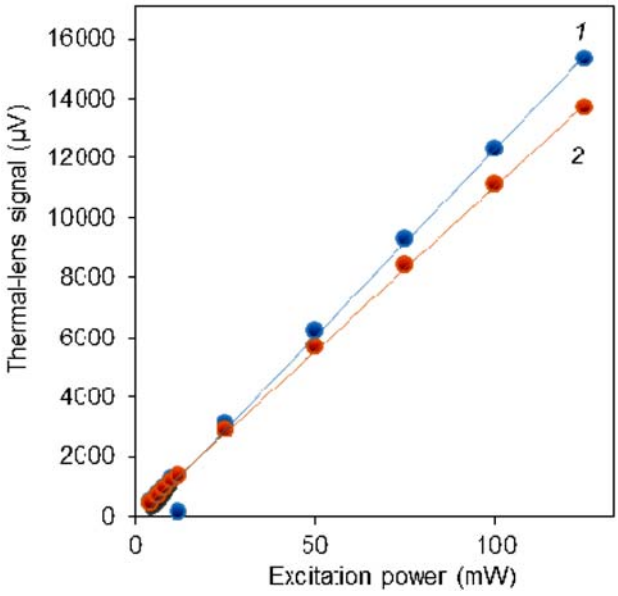

Figure 2. Dependence of the thermal-lens signal of Cr(VI) complex with diphenylcarbazide (4 μmol L^{-1}) on the power of the excitation laser light for two flow rates, (*1*) 5 μL min^{-1} and (*2*) 30 μL min^{-1}.

3. 2. The Effect of the Flow Rate

Apart from significantly lower amounts of the sample and reagents in a microfluidic chip, another advantage of μFIA–TLM is the implementation of fast detection of a large number of samples (or even real-time monitoring) with a high throughput.[27,38] However, this requires that the time of analysis of a single sample is as low as possible, while retaining high sensitivity, i.e. the degree of completion of the photometric reaction should be high enough. On the other hand, the photodegradation of the reaction products does not allow lowering flow rates. Thus, the flow rate should be optimized to enable the completion of the complexation reaction between Cr(VI) and diphnylcarbazide and to decrease the effect of photodegradation. This can be achieved by varying the flow rate and by shifting the detection position downstream from the junction point of carried and reagent channels on the microchip.

However, flow rate requires a careful optimization. On one hand, at high flow rates, the reaction may not be complete, and the procedure sensitivity will be governed by the degree of completion. In addition, at high flow rates, peak shape may be distorted due to changes in mixing conditions, and this is very well known in macro-scale FIA. However, there is another reason of optimization, which is connected with the thermal-lens effect itself. The classical theory of this effect in large-scale samples predicts a decrease in the signal with an increase of the flow rate (the heated zone with thermal lens is removed with the flow away from the detection point, thus decreasing the signal).[39] In microfluidic chips and capillaries, the plots of the signal amplitude on the flow rate show a shape with a rather distinct maximum.[40–42] This is accounted for by the fact that heating and cooling at high modulation frequencies do not result in complete dissipation of the heat during the cooling half-period of measurements, and the incremental heating during a measurement cycle is lower than in the case of complete dissipation of heat. At low flow rates, the flow removes this residual heating at the end of the measurement cycle, the incremental heating governing the signal increases, and signal grows up. At higher flow rates, the effects of the flow also affect the heating and the signal start to decrease like in the case of macro-scale flows in thermal lensing.[43]

In this study, we obtained the results expected from the viewpoint of this heating model and based on our previous findings.[34,42] For the modulation frequency of 1 kHz, the dissipation time (half-period of the cycle when the excitation beam is closed by the chopper) is 500 μs. The thermal behaviour of a thermal-lens experiment is governed by the characteristic time constant of the thermal lens, $t_c = \omega$ where ω is the excitation beam radius and D_T is the thermal diffusivity. For the experimental conditions (excitation beam radius of 2 μm and an aqueous solution t_c is 7 μs. Thus, both heating and cooling half-cycles span for *ca.* $70t_c$. The heating period is long enough for attaining the thermal equilibrium (usually $50t_c$), however, the cooling half-cycle is governed by thermal effusivity and requires a longer time for the total dissipation of the thermal profile (*ca* $100t_c$).[39,42] These conditions can be attained by selecting lower modulation frequencies (which decrease the S/N ratio)[39] or switching to the asynchronous mode (heating and cooling half-cycles are independent), which is not always advantageous for fast in-flow measurements and cannot be based on lock-in schemes.[44] Thus, for a 1 kHz modulation frequency and a lock-in detection, a maximal S/N is obtained for given optical scheme.

Also, under these selected experimental conditions (pump beam size 4 μm, frequency 1 kHz, and flow rate larger than 5 μL/min), flow-induced decrease and increase are not based on incremental heating only. The signal increase for flow rates 5–10 μL min^{-1} (Fig. 3) is also due to the less photodegradation, while less Cr-DPC diffusion into the area irradiated by the excitation beam[45] contributes to an additional signal decrease at higher flow rates. As Fig. 2 shows, there is about a 20% contribution from the photodegradation when comparing 5 μL min^{-1} to flows as high as 30 μL min^{-1}. This 20% contribution is close to the observed increase in TLS signal with the flow rate at 10 μL min^{-1} (25%), and not much further improvement can be expected. Therefore, measurements at many different flow rates were not needed. The position of this maximum depends on other optimization parameters only slightly. This optimum flow rate was observed for both microchips N1 and N2. In the following experiments, the flow rate was set to 10 μL min^{-1}.

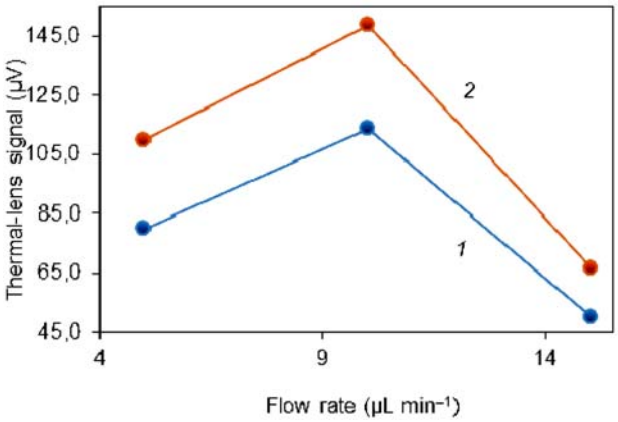

Figure 3. Dependence of the thermal-lens signal of Cr(VI) (4 μmol L^{-1}) complex with diphenylcarbazide (20 μmol L^{-1}) on the flow rate for two injection volumes of the reagent (*1*) 0.9 μL and (*2*) 1.4 μL, the detection distance from the mixing point, 29 cm; excitation power, 100 mW.

3. 3. The Effect of the Detection Distance from the Junction Point

After optimizing two key parameters directly governing the sensitivity of thermal-lens measurements, we moved on to the optimization of the flow reaction parameters. The time of molecular diffusion equals L^2/D (L is the characteristic distance and D is the diffusion coefficient, respectively) in microfluidic chips is usually several seconds for L= 100 μm and $D = 10^{-5}$ cm^2 s^{-1}. The specific interface area $\sigma = S/V \propto 1/L$ (S is the surface area and V is the channel volume) is *ca.* 100 cm^{-1}. Compared to cells with path lengths of 1 cm, low diffusion times and higher specific interface area provide a significant increase in the reaction rate.[46–53] Thus, we determined the optimum time of the reaction by varying the position of the thermal-lens detection against the junction point in the microchip. It was found that for all the injection volumes and flow rates, the peak height first increases up to the detection position of 10 cm and then decreases by 10–20% on a further increase in the detection position (Fig. 4).

An increase in the signal is due to an increase in the degree of completion of the reaction between Cr(VI) and DPC, while the further decrease is due to peak washout

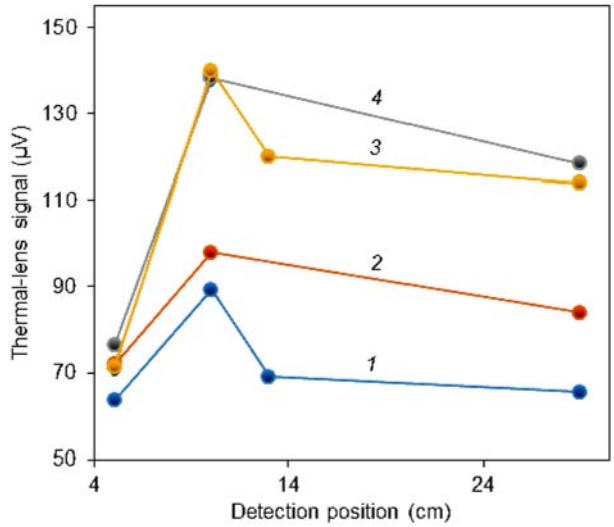

Figure 4. Dependence of the thermal-lens signal of Cr(VI) (4 μmol L^{-1}) complex with diphenylcarbazide (20 μmol L^{-1}) for various flow rates and injection volumes of the reagent (1) V = 0.6 μL and q = 10 μL min^{-1}; (2) V = 0.6 μL and q = 5 μL min^{-1}; (3) V = 0.9 μL and q = 10 μL min^{-1}; (4) V = 0.9 μL and q = 5 μL min^{-1}; excitation power, 100 mW.

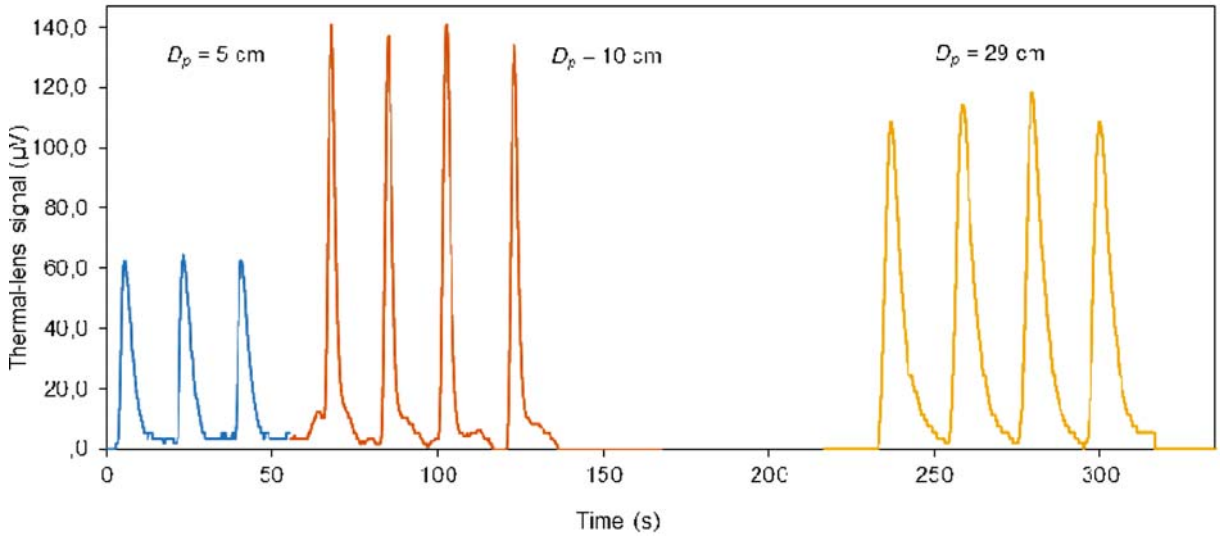

Figure 5. Shapes of the thermal-lens signal of Cr(VI) (4 μmol L^{-1}) complex with diphenylcarbazide (20 μmol L^{-1}) for various positions of the detector from the mixing point; flow rate, 10 μL min^{-1}, injection volume of the reagent, 0.9 μL; excitation power, 100 mW.

due to diffusion and, to a lesser degree, due to the advection by fluid flow of the formed chelate in the channel. Washout results in an increase in the peak width, which can be clearly seen in Fig. 5. Contrary to the peak height, peak areas increase and reach a plateau at the position of the detection position from the mixing point (junction of carrier and reagent channels) of 10 cm (Fig. 5), which corresponds to the maximum peak height. This means that the reaction is close to completion when the peak areas cease to change. Thus, the optimum detection position was selected as 10 cm from the mixing point. Under these conditions, the peak height linearly depends on chromium concentration, thus this parameter was used as the analytical signal for the quantification of Cr(VI).

3. 4. The Effect of the Injected Volume

The flow of the resulting chromium chelate in a microchannel is rather fast compared to the detection zone with a cross-section of several square micrometers; thus, the residence time of a sub-microliter sample at the detection position is 2–3 s at a flow rate of 15 μL min^{-1}. Therefore, as the reagent is injected into the continuous flow of the test sample, the injected volume may be a significant parameter of the sensitivity of the determination.

Figure 6 shows dependences of the peak height in the injected volume of the reagent under several detection positions. It shows that the dependence of the signal on the injected volume is not affected by the location of detection position with respect to the point of mixing. However, flow rates of 5 and 10 μL min^{-1} show slightly different behavior. For a flow rate of 5 μL min^{-1}, signal first increases and then decreases with an increase in the injected volume. This correlates with the existing data,[34,54] and is accounted for by the lack of the reagent at low injected volumes for the formation of the chelate with all the metal in the chelation zone.

An increase in the injection time (and volume) provides a higher concentration of the chelate, however, at some point, the washout of the sample zone at high injection volume results in the decrease in the peak height. In addition, an increase in the injected volume distorts the peak shapes (Fig. 7).

At a flow rate of 10 μL min^{-1}, the rate of injection can be increased, which provides lower washout of the injection zone (Fig. 7). Thus, the curves in Fig. 6 (b) show no decrease in the signal at longer detection positions for the given range of the injection volume (0.4–1.4 μL), while a signal decrease was observed with a further increase in the injection volume (such as the signals for $V \geq 1.6$ μL in Fig. 7 (b)). Moreover, the curves for the detection positions of 10 and 29 cm from the junction of carrier and reagent channels are very similar. The dependence of the signal on the injection volume of the reagent does not depend on the excitation power. Thus, for the selected flow rate of 10 μL min^{-1} we used the injection volume of 1.4 μL.

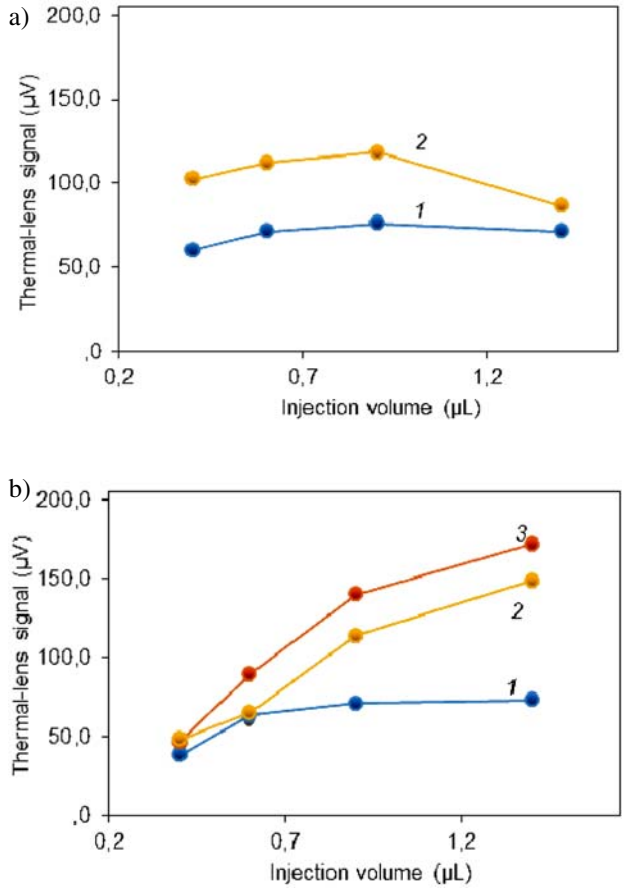

Figure 6. Dependence of the thermal-lens signal of Cr(VI) (4 μmol L^{-1}) complex with diphenylcarbazide (20 μmol L^{-1}) on the injection volume of the reagent for various detection positions from the mixing point: flow rate, (a) 5 μL min^{-1}, *1*, D_p = 5 cm and *2*, D_p = 29 cm and (b) 10 μL min^{-1}, *1*, D_p = 5 cm, *2*, D_p = 10 cm, and *3*, D_p = 29 cm; excitation power, 100 mW.

3. 5. Performance Parameters for Cr(VI)

Under the optimized conditions (Table 2) we built calibration plots for Cr(VI) concentrations between 5 ng mL^{-1} and 50 μg mL^{-1}.

The calibration equation under these conditions is

$H = (2.34 \pm 0.04) \times 10^8 c + (0.5 \pm 0.2)$,

$r = 0.9982$; $P = 0.95$, $n = 33$

The limit of detection of Cr(VI) is 15 ng mL^{-1} (2.9×10^{-7} mol L^{-1}), which correlates well with previously re-

Table 2. The optimum conditions for the determination of Cr(VI) with DPC by μFIA–TLM (excitation wavelength, 514.5 nm; excitation power, 100 mW)

Parameter	Value
Detection distance, downstream from the junction point of the microchip	10 cm
Flow rate	10 μL min^{-1}
Injection volume	1.4 μL

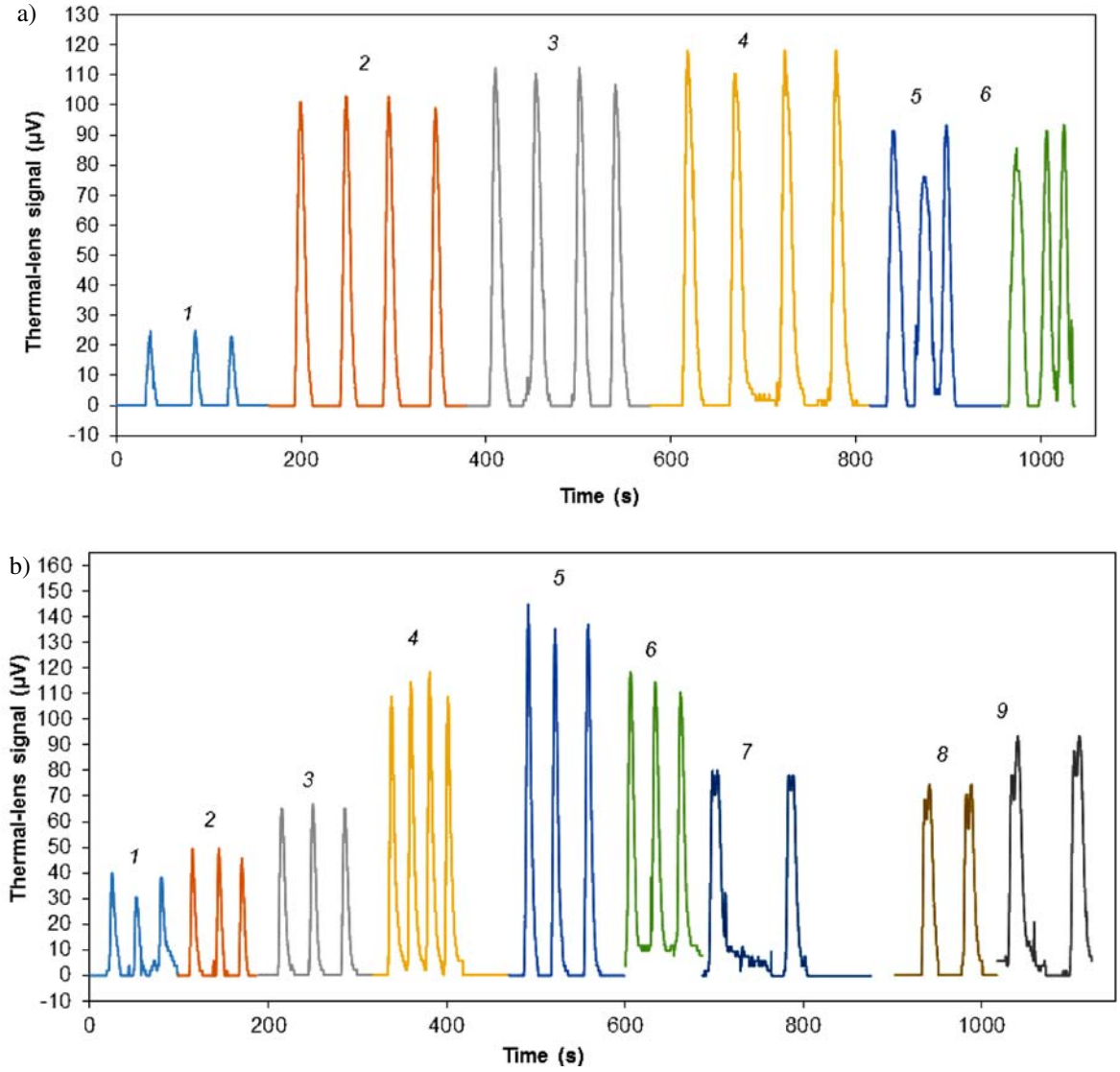

Figure 7. Shapes of thermal-lens signal (with the subtracted background signal) of Cr(VI) (4 μmol L-1) complex with diphenylcarbazide (20 μmol L-1) for various conditions:
(a) flow rate, 5 μL min-1, detection position, 29 cm from the mixing point (1, V = 0.2 μL, 2, V = 0.4 μL, 3, V = 0.6 μL, 4, V = 0.9 μL, 5, V = 1.4 μL, and 6, V = 1.6 μL)
(b) flow rate, 10 μL min-1, detection position, 29 cm from the mixing point (1, V = 0.2 μL, 2, V = 0.4 μL, 3, V = 0.6 μL, 4, V = 0.9 μL, 5, V = 1.4 μL, 6, V = 1.6 μL; 7, V = 2.0 μL; 8, V = 2.2 μL; and 9, V = 2.5 μL.

ported value[34] when taking into account 200 times shorter optical interaction length and the same excitation power. The linear range, 40 ng mL^{-1}–10 μg mL^{-1} is wider compared to previous findings.[34] The relative standard deviation in the range 0.1–1 μg mL^{-1} is no higher than 0.1.

Thus, the proposed procedure developed for a specially designed microchip corresponds to the required sensitivity level for microfluidic applications.[1,2] At a flow rate of 10 μL min^{-1}, the time required for a single injection of the reagent (optimum injection volume) is 10 s, i.e. the reagent can be injected 6 times per minute. That means 360 analyses per hour for continuous and approximately 180 for discrete analysis. It is noteworthy that this time is almost fivefold lower compared to the analysis time in FIA–TLS for the optimum flow rate of 2.5 mL min^{-1}.

4. Conclusions

Thus, we succeeded in the miniaturization of the detection scheme for the determination of trace chromium(VI) and developed a μFIA–TLM procedure for the injection of the preconditioned reagent into a continuous or discrete flow of the test analyte solution. We focused on the optimization for the conditions of the reaction of Cr(VI)

with diphenylcarbazide in the flow in a microfluidic chip specially designed for the target reaction.[34] Such an optimization in a microflow is very simple and non-laborious and provides good sensitivity. We believe that this will facilitate developing the procedures and applications for compact thermal-lens instruments and in turn, stimulate developing such instruments. This will undoubtedly expand the arsenal of analytical methods in the field of trace analysis.

5. Acknowledgments

We thank the Slovenian Research Agency for the financial support through the grant P1-0034, and M. Liu acknowledges the support from EU Social fund and the Ministry of Education, Science and Sport of the Republic of Slovenia through the Grant 3330-14-509065. M. Proskurnin acknowledges partial support from the Russian Foundation for Basic Research, grants nos. 13-03-00535a and 16-03-01089.

6. References

1. D. Q. Zou, Y. Qing, Y. T. Li, M. S. Liu and Y. L. Yang, *J. Iran Chem. Soc.*, **2014**, *11*, 415–422. http://dx.doi.org/10.1007/s13738-013-0313-6
2. J. P. Wise, J. T. F. Wise, C. F. Wise, S. S. Wise, C. Gianios, H. Xie, W. D. Thompson, C. Perkins, C. Falank and J. P. Wise, *Environ. Sci. Technol.*, **2014**, *48*, 2997–3006. http://dx.doi.org/10.1021/es405079b
3. M. Feki-Tounsi, P. Olmedo, F. Gil, M. N. Mhiri, A. Rebai and A. Hamza-Chaffai, *Environ. Sci. Pollut. Res.*, **2014**, *21*, 11433–11438. http://dx.doi.org/10.1007/s11356-014-3099-x
4. E. C. Alexopoulos, X. Cominos, I. P. Trougakos, M. Lourda, E. S. Gonos and V. Makropoulos, *Bioinorg. Chem. Appl.*, **2008**. http://dx.doi.org/10.1155/2008/420578
5. J. L. Parks, L. McNeill and M. Edwards, *Talanta*, **2014**, *130*, 226–232. http://dx.doi.org/10.1016/j.talanta.2014.06.052
6. H. Peng, N. Zhang, M. He, B. Chen and B. Hu, *Talanta*, **2015**, *131*, 266–272. http://dx.doi.org/10.1016/j.talanta.2014.07.054
7. N. Suksomboon, N. Poolsup and A. Yuwanakorn, *J. Clin. Phar. Ther.*, **2014**, *39*, 292–306. http://dx.doi.org/10.1111/jcpt.12147
8. N. N. Meeravali, R. Manjusha and S. J. Kumar, *J. Anal. At. Spectrom.*, **2014**, *29*, 2168–2175. http://dx.doi.org/10.1039/C4JA00206G
9. A. G. Cox and C. W. McLeod, *Anal. Chim. Acta*, **1986**, *179*, 487–490. http://dx.doi.org/10.1016/S0003-2670(00)84497-9
10. Y. Li, N. K. Pradhan, R. Foley and G. K. C. Low, *Talanta*, **2002**, *57*, 1143–1153. http://dx.doi.org/10.1016/S0039-9140(02)00196-0
11. B. L. Batista, D. Grotto, J. L. Rodrigues, V. C. de Oliveira Souza and F. Barbosa Jr, *Anal. Chim. Acta*, **2009**, *646*, 23–29. http://dx.doi.org/10.1016/j.aca.2009.05.022
12. Y. Xiang, L. Mei, N. Li and A. Tong, *Anal. Chim. Acta*, **2007**, *581*, 132–136. http://dx.doi.org/10.1016/j.aca.2006.08.006
13. W. Yao and R. H. Byrne, *Talanta*, **1999**, *48*, 277–282. http://dx.doi.org/10.1016/S0039-9140(98)00243-4
14. J. Ma, D. Yuan and R. H. Byrne, *Environ. Monit. Assess.*, **2013**, *186*, 367–373. http://dx.doi.org/10.1007/s10661-013-3381-2
15. J. Xin, Y. He, J. Hu, Y. Duan and X. Hou, *Spectrosc. Lett.*, **2009**, *42*, 351–355. http://dx.doi.org/10.1080/00387010903185728
16. Y. Wang, M. Huang, X. Guan, Z. Cao, F. Chen and X. Wang, *Opt. Express*, **2013**, *21*, 31130–31137. http://dx.doi.org/10.1364/OE.21.031130
17. M. A. Rzetala, *Soil. Sediment. Contam.*, **2015**, *24*, 49–63. http://dx.doi.org/10.1080/15320383.2014.911721
18. B. Bocca, A. Pino, A. Alimonti and G. Forte, *Regul. Toxicol. Pharm.*, **2014**, *68*, 447–467. http://dx.doi.org/10.1016/j.yrtph.2014.02.003
19. A. Otag, M. Hazar, I. Otag, A. C. Gurkan and I. Okan, *Globa J. Health Sci.*, **2014**, *6*, 90–
20. S. Doker, M. Hazar, M. Uslu, I. Okan, E. Kafkas and Bosgelmez, II, *Biol. Trace Elem. Res.*, **2014**, *158*, 15–21. http://dx.doi.org/10.1007/s12011-014-9912-z
21. J. Mairhofer, K. Roppert and P. Ertl, *Sensors*, **2009**, *9*, 4804–4823. http://dx.doi.org/10.3390/s90604804
22. B. C. Giordano, D. S. Burgi, S. J. Hart and A. Terray, *Anal. Chim. Acta*, **2012**, *718*, 11–24. http://dx.doi.org/10.1016/j.aca.2011.12.050
23. K. Mawatari, T. Tsukahara, Y. Tanaka, Y. Kazoe, P. Dextras and T. Kitamori, *Extended-Nanofluidic Systems for Chemistry and Biotechnology*, Imperial College Press, London, **2012**. http://dx.doi.org/10.1142/p813
24. T. Yamamoto, Y. Kazoe, K. Mawatari and T. Kitamori, *J. Synth. Org. Chem. Jpn.*, **2011**, *69*, 526–533. http://dx.doi.org/10.5059/yukigoseikyokaishi.69.526
25. V. S. Dudko, A. P. Smirnova, M. A. Proskurnin, A. Hibara and T. Kitamori, *Russ. J. Gen. Chem.*, **2012**, *82*, 2146–2153. http://dx.doi.org/10.1134/S1070363212120341
26. K. Mawatari, T. Ohashi, T. Ebata, M. Tokeshi and T. Kitamori, *Lab Chip*, **2011**, *11*, 2990–2993. http://dx.doi.org/10.1039/c1lc20175a
27. M. Liu and M. Franko, *Crit. Rev. Anal. Chem.*, **2014**, *44*, 328–353. http://dx.doi.org/10.1080/10408347.2013.869171
28. M. Liu and M. Franko, *Int. J. Thermophys.*, **2014**, *35*, 2178–2186. 10.1007/s10765-014-1714-1 http://dx.doi.org/10.1007/s10765-014-1714-1
29. M. Šikovec, M. Novic and M. Franko, *J. Chromatogr. A*, **1996**, *739*, 111–117. http://dx.doi.org/10.1016/0021-9673(96)00054-4
30. M. Šikovec, M. Franko, F. G. Cruz and S. A. Katz, *Anal. Chim. Acta*, **1996**, *330*, 245–250. http://dx.doi.org/10.1016/0003-2670(96)00175-4
31. M. Šikovec, F. G. Cruz, M. Franko and S. A. Katz, *Spectrosc. Lett.*, **1996**, *29*, 465–475.

http://dx.doi.org/10.1080/00387019608006664
32. M. Šikovec, M. Franko, M. Novic and M. Veber, *J. Chromatogr. A*, **2001**, *920*, 119–125. http://dx.doi.org/10.1016/S0021-9673(01)00611-2
33. M. Šikovec, M. Novic and M. Franko, *Ann. Chim. (Rome)*, **2000**, *90*, 163–168.
34. A. Madzgalj, M. L. Baesso and M. Franko, *Eur. Phys. J. Special Topics*, **2008**, *153*, 503–506. http://dx.doi.org/10.1140/epjst/e2008-00494-4
35. M. Liu and M. Franko, *Appl. Phys. B*, **2014**, *115*, 269–277. http://dx.doi.org/10.1007/s00340-013-5601-4
36. *ISO/IEC 17025:2005 General requirements for the competence of testing and calibration laboratories*, ISO/IEC**2005**.
37. M. Liu, U. Novak, I. Plazl and M. Franko, *Int. J. Thermophys.*, **2014**, *35*, 2011–2022. http://dx.doi.org/10.1007/s10765-013-1515-y
38. C. L. Cassano, K. Mawatari, T. Kitamori and Z. H. Fan, *Electrophoresis*, **2014**, *35*, 2279–2291. http://dx.doi.org/10.1002/elps.201300430
39. S. E. Bialkowski, *Photothermal spectroscopy methods for chemical analysis*, Wiley-Interscience, New York, **1996**.
40. S. N. Bendrysheva, M. A. Proskurnin, U. Pyell and W. Faubel, *Anal. Bioanal. Chem.*, **2006**, *385*, 1492–1503. http://dx.doi.org/10.1007/s00216-006-0602-3
41. N. Ragozina, S. Heissler, W. Faubel and U. Pyell, *Anal. Chem.*, **2002**, *74*, 4480–4487. http://dx.doi.org/10.1021/ac020095i
42. A. Smirnova, M. A. Proskurnin, S. N. Bendrysheva, D. A. Nedosekin, A. Hibara and T. Kitamori, *Electrophoresis*, **2008**, *29*, 2741–2753. http://dx.doi.org/10.1002/elps.200700914
43. M. A. Proskurnin, S. N. Bendrysheva, N. Ragozina, S. Heissler, W. Faubel and U. Pyell, *Appl. Spectrosc.*, **2005**, *59*, 1470–1479. http://dx.doi.org/10.1366/000370205775142494
44. M. A. Proskurnin, D. S. Volkov, T. A. Gor'kova, S. N. Bendrysheva, A. P. Smirnova and D. A. Nedosekin, *J. Anal. Chem. (Russ.)*, **2015**, *70*, 249–276. http://dx.doi.org/10.1134/S1061934815030168
45. P. R. B. Pedreira, L. R. Hirsch, J. R. D. Pereira, A. N. Medina, A. C. Bento, M. L. Baesso, M. C. Rollemberg, M. Franko and J. Shen, *J. Appl. Phys.*, **2006**, *100*, 044906. http://dx.doi.org/10.1063/1.2245201
46. G. J. M. Bruin, *Electrophoresis*, **2000**, *21*, 3931–3951. http://dx.doi.org/10.1002/1522-2683(200012)21:18<3931::AID-ELPS3931>3.0.CO;2-M
47. C. Maims, J. Hulme, P. R. Fielden and N. J. Goddard, *Sens. Actuat. B*, **2001**, *77*, 671–678. http://dx.doi.org/10.1016/S0925-4005(01)00773-0
48. C. Yi, C.-W. Li, S. Ji and M. Yang, *Anal. Chim. Acta*, **2006**, *560*, 1–23. http://dx.doi.org/10.1016/j.aca.2005.12.037
49. J. H. Min and A. Baeumner, *J. Ind. Eng. Chem.*, **2003**, *9*, 1–8.
50. K. B. Mogensen, H. Klank and J. P. Kutter, *Electrophoresis*, **2004**, *25*, 3498–3512. http://dx.doi.org/10.1002/elps.200406108
51. S. D. Minteer, *Microfluidic techniques: reviews and protocols*, Humana Press, Totowa, N.J., **2006**.
52. M. Tokeshi, Y. Kikutani, A. Hibara, K. Sato, H. Hisamoto and T. Kitamori, *Electrophoresis*, **2003**, *24*, 3583–3594. http://dx.doi.org/10.1002/elps.200305661
53. P. C. H. Li, *Microfluidic lab-on-a-chip for chemical and biological analysis and discovery*, CRC Press, Taylor & Francis Group, Boca Raton, **2006**.
54. M. A. Proskurnin, V. V. Chernysh and M. A. Kurzin, *J. Anal. Chem. (Russ.)*, **2001**, *56*, 31–35. http://dx.doi.org/10.1023/A:1026711310778

Povzetek

Za določanje šestvalentnega kroma [Cr(VI)] s pretočno injekcijsko analizo v mikrofluidnem sistemu (μFIA) in detekcijo z mikroskopijo na osnovi toplotnih leč, smo izbrali optimalne reakcijske pogoje za interakcijo Cr(VI) s kolorimetričnim reagentom difenilkarbazidom. Glavna značilnost uporabljenega pretočnega sistema je injiciranje reagenta v nosilni tok, ki vsebuje analit. To, ob stalnem pretoku vzorca skozi mikročip, v praksi omogoča kontinuirni monitoring Cr(VI) v realnem času. Pri izbranih pogojih (vzbujevalna valovna dolžina 514,5 nm, moč vzbujanja 100 mW, točka detekcije 10 cm po točki mešanja, pretok 10 μL min^{-1}, injicirani volumen 1,4 μL) smo dosegli mejo zaznave 15 ng mL^{-1} ($2,9 \times 10^{-7}$ mol L^{-1}). Pri tem je bilo območje linearnosti 40 ng mL^{-1} – 10 μg mL^{-1}, relativni standardni odmik v koncentracijskem območju 0.1–1 μg mL^{-1} pa manjši od 10 %. Opisani sistem omogoča kontinuirno merjenje koncentracije Cr(VI) s 360 analizami na uro.